RSC Advances

ROYAL SOCIETY OF CHEMISTRY

www.rsc.org/advances

Structural Change of Graphene Oxide in Methanol Dispersion

Flavio Pendolino,*[a] Giovanni Capurso,[b] Amedeo Maddalena,[b] and Sergio Lo Russo[a]

Received Xth XXXXXXXXXX 20XX, Accepted Xth XXXXXXXXX 20XX
First published on the web Xth XXXXXXXXXX 200X
DOI: 10.1039/b000000x

Graphene oxide is derivative graphene material containing oxygen domains. Its debatable structure depends on the specific functional groups bonded to the graphene basal plane which impacts on the graphene oxide reactivity. Here, we report the influence of the methanol solvent which affects the functionalization of the pristine graphene differently than water graphene oxide dispersion.

Since the early study on graphene by Geim and Novoselov[1], remarkable attention was captured by this carbon allotrope and its functionalization for a future application in electronic devices. Among the graphene derivatives, graphene oxide (GO) attracted attention as a novel carbonaceous material with noticeably features. Graphene oxide (GO) consists of a 2D nanographene flake decorated with oxygen domains. An amphiphilic character is derived by the large central domain of graphene, while the bonded oxygen atoms confer a hydrophilic behaviour. The presence of oxygen domains imply profound implications in the reactivity of this material which has raised significant interest in several fields and applications such as conductive films[2], production of hydrogen[3], energy storage systems[4], emulsifying organic solvents for industrial processes[5] or biosensors[6]. The dispersion of GO in water is supposed to be kinetically stable[7–10], and the use of various solvents results in a different solubility, only. Nevertheless, polar solvents interact with GO producing a different structure which modifies the interaction with a target molecule. Because of the complexity of the GO *"molecule"*, a fundamental understanding is needed in order to describe the appropriate interaction process.

The present communication focuses on the fundamental issue regarding the controversial structure of the graphene oxide. The change of GO structure is discussed for GO dispersions into a polar medium, such as methanol and water. These results demonstrate that the GO functionalization is not exclusively due to the synthetic method, but depends on the effect of the solvent which modifies the functional groups on graphene basal plane and consequently its reactivity.

[a] *Department of Physics and Astronomy, University of Padova, via Marzolo 8, 35131 Padova, Italy; E-mail: flavio.pendolino@unipd.it*
[b] *Department of Industrial Engineering, University of Padova, via Marzolo 9, 35131 Padova, Italy*

The GO material, synthesised using a modified Sun's protocol[11], was placed in three flasks (30 mg GO / 7 ml solvent) and dispersed in methanol (GO−Met), distilled water (GO−H_2O) and 1:1 methanol/water (GO−Mix) to study the influence of the solvent. In the water dispersion, GO minimised the interactions with the solvent forming floating particles, as in surfactant solutions[12] (Fig. 1). In contrast, when a different polar solvent is used, *i.e.* methanol, the interaction with hydrophobic plane of graphene is allowed and the exfoliation process is improved. In fact, the methanol dispersion (GO−Met) appears as yellow crystal solution, while 1:1 methanol/water (GO−Mix) and water (GO−H_2O) dispersions turn to darker suspension with floating black particles. Negligible amount of precipitate is present in the fresh GO−Met dispersion; conversely, water leads to the formation of solid black precipitate. Therefore, the use of methanol enables to exfoliate graphene oxide more efficiently than water. Thus, the solubility for fresh GO dispersions is evaluated in 0.34 ± 0.06 g/L (GO−Met), 0.2 ± 0.04 g/L (GO−Mix) and 0.18 ± 0.04 g/L (GO−H_2O). In order to verify the formation of the GO flakes after dispersion in polar medium, X-ray diffractions were performed on the dry GO dispersions, as shown in Fig. 2. The expanded graphite pattern is reported as a reference, showing a characteristic narrow peak at $2\theta = 26.5°$. All the GO dispersions have a peak centred at $2\theta = 11.2°$ (main diffraction peak) and a wide peak in the range 15-35°. The position of maximum diffraction peak for GO is reported in the range $9-12°$ [3,13–16], in agreement with our result. These values are associated with the variation of the interlayer distance (d = 0.8 nm) in the GO dry sample due to the presence of chemical groups onto graphene basal plane. Concerning the broadness of the main peak for the GO dispersions, Lee et al.[13] reported that it is originated by the distribution of the amorphous coexistent phases. Furthermore, the solubilisation of GO in methanol leads to a reasonable little amount of unreacted graphite or multilayer graphene, producing a stochastic distribution of GO flakes on the XRD sample holder. The wide peak 15-35° exhibits two broad weak peaks at 22.2° and 26.2°, as we can see in the inset of Fig. 2. Typically, the presence of those wide peaks is not taken into consideration as characteristic peak of GO and often is omitted from the description of the GO X-ray analysis. As reported by Shin et

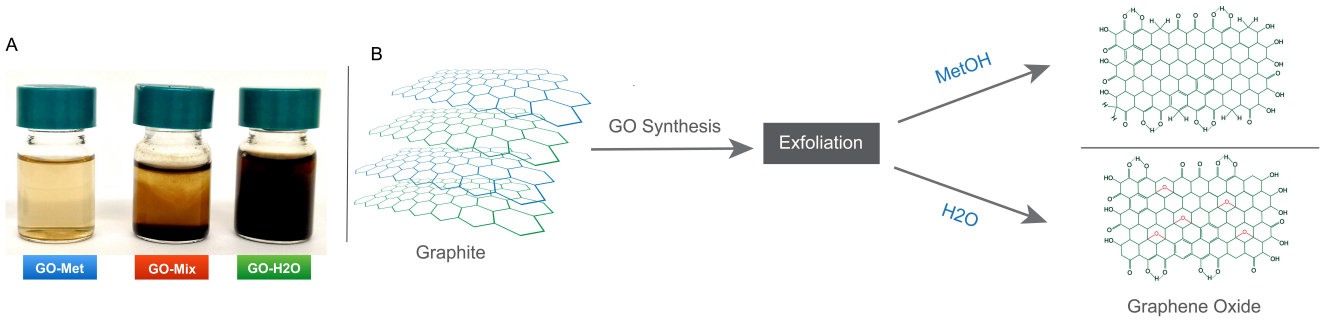

Fig. 1 (A) Digital camera image of GO dispersed in methanol (GO−Met), 1:1 methanol/water (GO−Mix) and in distilled water (GO−H_2O) after 5 minutes shaking (no sonication, waiting unshaken for 2 hours). (B) Illustration shows a schematic synthesis of GO and the structure for GO dispersed in methanol or water.

al.[17], the reduction of GO shows an X-ray peak around 24° while the GO main peak at 11° disappears when the amount of reducing agent ($NaBH_4$) is increased. Taking into account this facts, the peak at 22.2° may be related to the formation of reduced graphene oxide. Instead, the peak at 26.2° could be attributed to the multilayers graphene where the interlayer distance is still similar to the graphite (d = 0.34 nm). To understand the effect of the solvent on the modification of the functional groups bonded to the graphene basal plane, the GO dispersions (supernatants and precipitates) are investigated by means of Fourier-Transformed Infrared (FTIR). In Fig. 3 is reported FTIR spectra showing a structural change when the polarity of the solvent is varied. Spectra a-c show characteristic broad band of GO centred 3410 cm^{-1} corresponding to the stretching vibrations of bonded O−H. The doublet peaks (very weak) at 2922 cm^{-1} and 2945 cm^{-1} correspond to the symmetric and antisymmetric stretching vibrations of $-CH_2$. The peak corresponding to the C=O stretching vibration at 1730 cm^{-1} can also be found. Often, this band is related to the vibrations of the COOH group[3,13–16,18]. The peak at 1620 cm^{-1} is sometimes attributed to the O−H vibrations due to the presence of adsorbed water on the graphene basal plane[14]. Alternatively, this doublet can be attributed to a *keto-enol tautomeric equilibrium*. In the case of large molecules, where keto and enol groups are present, a tautomeric equilibrium between the keto and enol isomers occurs, *e.g.* as illustrated in the FTIR spectrum of acetylacetone[19]. From the relative intensity of the peaks at 1620 cm^{-1} and 1730 cm^{-1}, the tautomeric ratio is 1:1 for all the GO precipitates. The shoulder around 1375 cm^{-1} corresponds to the bending vibration of O−H. The stretching vibration for alcoholic C−OH in an aromatic six-membered ring is identified at 1228 cm^{-1}. This peak decreases its intensity when the water is used as solvent. The peak at 1060 cm^{-1} has a controversial interpretation. Some authors interpret this peak as the symmetric frequency related to the epoxy group. However, it is more reliable interpreting this vibration as the stretching of C−O for the primary alcohol in consistency with the presence of the wide peak around 3400 cm^{-1}. Generally, the interpretation of vibrations below 1000 cm^{-1} is difficult and subjected to several different interpretations, but in our experiments the very weak peaks found in GO−Met dispersion can be associated with aromatic systems.

The FTIR spectra for the supernatants are illustrated in the top panel in Fig. 3. It worth to note that the intensity of several peaks is changed and additional vibrations appeared with respect to the GO precipitate. The stretching vibration of $-CH_2$ (2921 cm^{-1} and 2850 cm^{-1}) becomes strong in GO−Met comparing with water GO dispersions. The supernatant dispersions has a different keto-enol tautomeric behaviour, showing a variation of the intensity of the peaks at 1620 cm^{-1} and at 1730 cm^{-1} when the polar solvent is changed. In water dispersion the ratio keto/enol is 1:1, while the intensity of the peak at 1620 cm^{-1} increases with the methanol content which indicates a shift of the tautomeric equilibrium to the enol form. This fact can be explained considering the effect of solvent on the keto-enol equilibrium. Generally, the polar solvents stabilise the keto tautomer which is more favoured when the dielectric constant is increased. By contrast, the tautomeric equilibrium is shifted to the enol form when hydrogen bonds are formed. In water dispersion, hydrogen bonds stabilise the enol form but, because the water has a higher dielectric constant (ε = 80), in comparison with methanol (ε = 33)[20], the keto form are present with an yield of 50%. In the spectrum *f*, the intense peak at 1620 cm^{-1}, provides an evidence to the shift of the tautomeric equilibrium to the enol form which is stabilised by the hydrogen bonds due to the methanol molecules and the low value of the dielectric constant. The interpretation of the peak at 1060 cm^{-1} as stretching vibration of C−OH is connected to the additional vibrations, found in spectrum *d*, which describe the asymmetric (1205 cm^{-1}) and

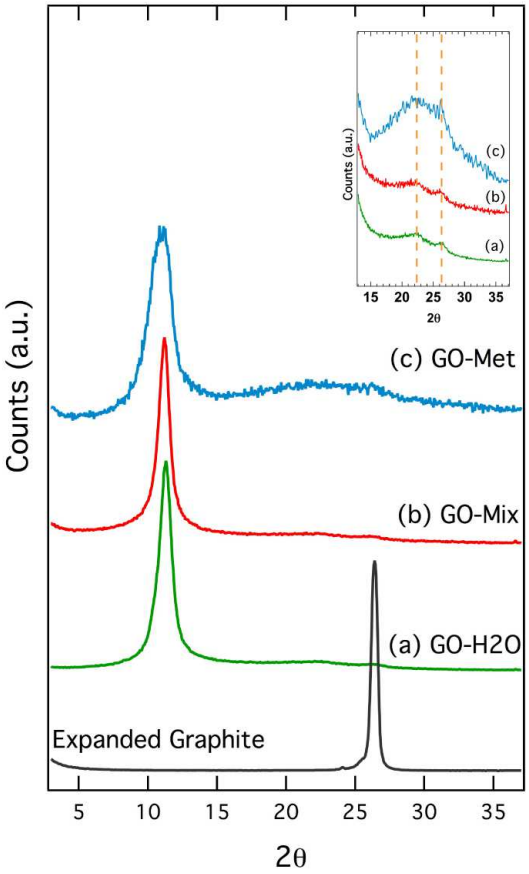

Fig. 2 X-ray diffraction patterns. GO dispersions, (*a*) GO−H_2O, (*b*) GO−Mix and (*c*) GO−Met, show a characteristic peak at 11.2°. The spectrum of the expanded graphite is reported as reference showing a sharp peak at 26.5°. Inset: the range 15-35° is expanded to show the two broad weak peaks at 22.2° and 26.2°.

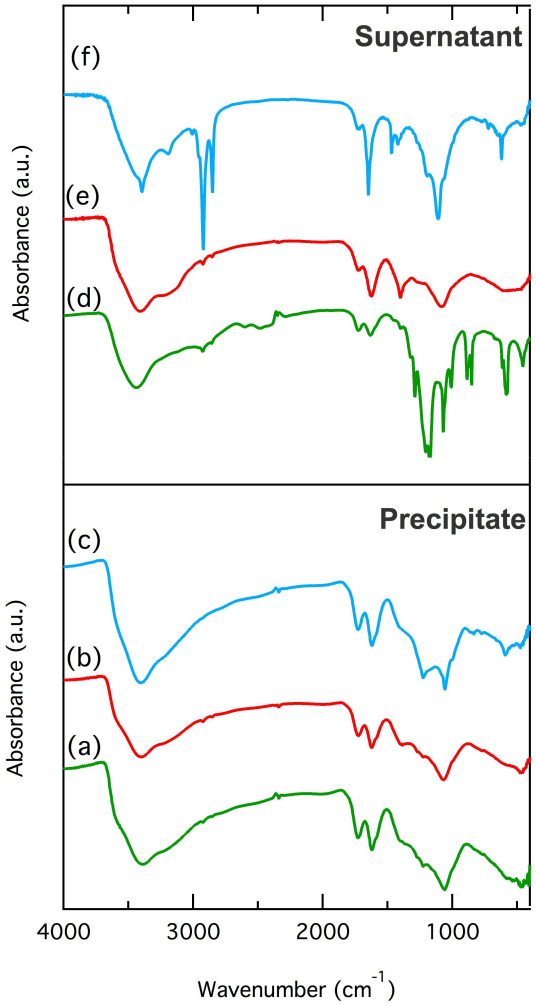

Fig. 3 FTIR spectra for GO. The green spectra (a,d) correspond to the GO−H_2O, red spectra (b,e) are GO−Mix and blue spectra (c,f) are GO−Met dispersions. Top panel (Supernatant) shows spectra for the liquid phase of GO solubilised in the solvent. Bottom panel shows spectra for the corresponding GO solid precipitates after the solubilisation.

symmetric (1170) C−O−C stretching for the epoxy group.

To investigate the presence of conjugated systems on the graphene basal plane, UV-vis experiments were performed on GO dispersed in polar solvents. Fig. 4 presents UV-vis spectra where any absorptions affect the region 400-900 nm. The variation of the UV-vis signal, among GO dispersions, occurs in the range 200-300 nm. The maximum absorbance takes place at 230 nm for all dispersions and it is attributed to $\pi \rightarrow \pi^{\star}$ transition which is due to the conjugated aromatic domains [18,21]. The intensity of this band is predominant for the GO−H_2O and GO−Mix dispersions which is an indication of the presence of an extended conjugate carbon system. The UV-vis analysis results in agreement with the FTIR conclusions demonstrating that the aromatic systems considerably contribute to the GO structure for water dispersions. The GO−Met supernatant dispersion does not show aromatic carbon rings in FTIR spectrum with the consequence that any UV-vis bands should appear close to 230 nm. Despite that, this band is revealed in the spectrum providing evidence of a conjugated system. The aromatic character can be associated to the presence of the enol isomer which forms an aromatic ring stabilised by hydrogen bonds. The aromatic ring is supported by the existence of an intense vibration at 1624 cm^{-1} in the FTIR spectrum for GO−Met dispersion. A shoulder is present at around λ = 290 nm and is often attributed to the $n \rightarrow \pi^{\star}$ transition of the carbonyl group. This band is kineti-

cally stable and shows at a constant wavelength value of 290 nm.

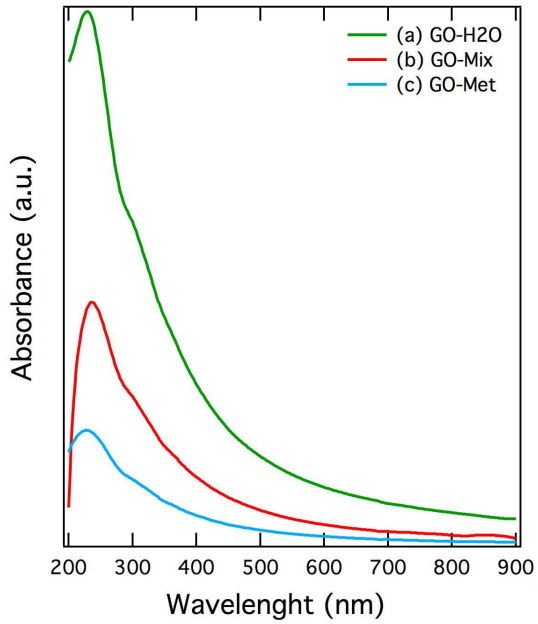

Fig. 4 UV-vis spectra of the GO dispersed in H_2O (a, green), 1:1 H_2O/MetOH (b, red) and MetOH (c, blue). The main band is centred at 230 nm with a shoulder around 290 nm.

In conclusion, we demonstrate that the structure of GO is affected by polar solvent, which does not act as a medium for solubilising the GO flakes, but an active interaction occurs between the graphene basal plane and the molecules of the solvent. The debatable presence of epoxy groups is discussed dealing with the interaction between graphene and water molecules. The keto-enol tautomerism explains both the presence of hydroxyl (−O−H) and carbonyl (−C=O) groups, as well as the aromatic character of the material. The presence of aromatic six-membered rings in the GO structure has been further confirmed also by UV-vis spectral analysis. The questionable GO structures are not only controlled by the used synthetic method, but the interaction with the polar solvent also contributed to alter the functional groups bonded to the graphene basal plane. The variety of structures and models, reported in literature, are the direct consequence of the misevaluation of the effect of the solvent on the GO functionalization. A further investigation suggests a modification of the GO structure with the time and a kinetic work is under study.

EXPERIMENTAL SECTION

Chemicals. The following chemicals were used as received: $KMnO_4$ (Sigma-Aldrich), H_2SO_4 (98%,Sigma-Aldrich), HCl (37%,Sigma-Aldrich), Expanded graphite ECOPHIT 50 (ECOPHIT). *Structural Characterisation.* Diffraction data were acquired with Bruker D8 Advance, Cu K_α radiation λ = 0.15418 nm. UV-vis spectra were recorded in Jasco V/570 spectrometer with quartz cell. FTIR measurements were carried out in Jasco FT/IR-620 spectrometer using KBr pellets. *Synthesis of Graphene Oxide*. The production of graphene oxide was carried out using a modified Sun's synthetic protocol which enhances the safety conditions[11]. Expanded graphite (5 g) and $KMnO_4$ (15 g) were introduced into 1L beaker and stirred until homogeneity. The beaker was placed in an ice-water bath and 100 ml of concentrated H_2SO_4 (98%) were added slowly (exothermic reaction) with continuous stirring until a petrol-green liquid paste was obtained. Then, the beaker was set to room temperature with a continuous stirring until a foam-like material was formed (about 20 min). At this stage, to raise the safety, the foam material was stirred to avoid possible density gradient which has dangerous effects during the solubilisation in water. Thus, the beaker was placed again in the ice-water bath and 400 ml distilled water were added very slowly avoiding uncontrolled temperature increase. The green-brownish liquid was placed in the 90°C water bath for 1 hour to obtain a dark suspension. The suspension was paper filtered and washed with 500 ml distilled water, 200 ml HCl 5% and 500 ml distilled water. The HCl solution served to remove manganese. The presence of sulfate ion was tested with a $BaSO_4$ spot test.

Acknowledgement

This work was funded by the University of Padova in the frame of the "Progetto Strategico MAESTRA".

References

1 K. S. Novoselov, A. K. Geim, S. V. Morozov, D. Jiang, Y. Zhang, S. V. Dubonos, I. V. Grigorieva and A. A. Firsov, *Science*, 2004, **306**, 666–669.
2 A. L. Higginbotham, D. V. Kosynkin, A. Sinitskii, Z. Sun and J. M. Tour, *ACS Nano*, 2010, **4**, 2059–2069.
3 T.-F. Yeh, J.-M. Syu, C. Cheng, T.-H. Chang and H. Teng, *Adv. Funct. Mater.*, 2010, **20**, 2255–2262.
4 J. Xu, K. Wang, S.-Z. Zu, B.-H. Han and Z. Wei, *ACS Nano*, 2010, **4**, 5019–5026.
5 L. J. Cote, J. Kim, V. C. Tung, J. Luo, F. Kim and J. Huang, *Pure Appl. Chem.*, 2011, **83**, 95–110.
6 Y. Liu, D. Yu, C. Zeng, Z. Miao and L. Dai, *Langmuir*, 2010, **26**, 6158–6160.
7 O. C. Compton and S. T. Nguyen, *Small*, 2010, **6**, 711–723.
8 Y. Si and E. T. Samulski, *Nano Lett.*, 2008, **8**, 1679–1682.
9 J. Kim, L. J. Cote and J. Huang, *Acc. Chem. Res.*, 2012, **45**, 1356–1364.

10 S. Stankovich, R. D. Piner, X. Chen, N. Wu, S. T. Nguyen and R. S. Ruoff, *J. Mater. Chem.*, 2006, **16**, 155–155.

11 L. Sun and B. Fugetsu, *Mater. Lett.*, 2013, **109**, 207–210.

12 R. Jalili, S. H. Aboutalebi, D. Esrafilzadeh, K. Konstantinov, J. M. Razal, S. E. Moulton and G. G. Wallace, *Mater. Horiz.*, 2013, **1**, 87–91.

13 D. W. Lee, L. De Los Santos, V, J. W. Seo, L. L. Felix, A. Bustamante D, J. M. Cole and C. H. W. Barnes, *J. Phys. Chem. B*, 2010, **114**, 5723–5728.

14 A. Kaniyoor, T. T. Baby and S. Ramaprabhu, *J. Mater. Chem.*, 2010, **20**, 8467–8469.

15 A. M. Dimiev and J. M. Tour, *ACS Nano*, 2014, **8**, 3060–3068.

16 B. Shen, D. Lu, W. Zhai and W. Zheng, *J. Mater. Chem. C*, 2013, **1**, 50–53.

17 H.-J. Shin, K. K. Kim, A. Benayad, S.-M. Yoon, H. K. Park, I.-S. Jung, M. H. Jin, H.-K. Jeong, J. M. Kim, J.-Y. Choi and Y. H. Lee, *Adv. Funct. Mater.*, 2009, **19**, 1987–1992.

18 H. Cao, X. Wu, G. Yin and J. H. Warner, *Inorg. Chem.*, 2012, **51**, 2954–2960.

19 Webbook Nist, *http://webbook.nist.gov/ (accessed June 2014)*.

20 SigmaAldrich, *http://www.sigmaaldrich.com/chemistry/solvents.html (accessed June 2014)*.

21 J. I. Paredes, S. Villar-Rodil, A. Martínez-Alonso and J. M. D. Tascón, *Langmuir*, 2008, **24**, 10560–10564.